J. Phys. Chem. A **2002,** *106,* 9930−9938

Keto−Enol Isomerization of Gas-Phase 2′-Methylacetophenone Molecular Ions Probed by High-Temperature Near-Blackbody-Induced Dissociation, Ion−Molecule Reactions, and ab Initio Calculations[†]

Tatiana Giroldo and José M. Riveros*

Instituto de Química, Universidade de São Paulo, Caixa Postal 26077, CEP 05513-970 São Paulo, SP, Brazil

Received: March 1, 2002; In Final Form: June 25, 2002

The thermal dissociation of several substituted acetophenone molecular ions induced by infrared radiation from a hot wire has been studied in a Fourier transform ion cyclotron resonance spectrometer. The temperature dependence of the dissociation rate constants reveals that the 2′-methylacetophenone molecular ion is characterized by a much higher activation energy for dissociation than other acetophenones. This molecular ion also exhibits a very different behavior with respect to charge-transfer reactions. Unlike molecular ions obtained from other isomeric acetophenones, the 2′-methylacetophenone $M^{+\bullet}$ ion does not promote charge exchange with dimethyl disulfide but does undergo relatively slow electron transfer with ferrocene (IE = 6.74 eV). Ab initio calculations at the MP2/6-31G(d) level predict that the $2\text{-}MeC_6H_4COCH_3^{+\bullet}$ ion (**1**) can undergo facile tautomerization to the much more stable enol ion **2**, $2'\text{-}{\bullet}CH_2C_6H_4C^+(OH)CH_3$, by a 1,4-hydrogen migration (calculated energy barrier of 20 kJ mol^{-1}). The calculated recombination energy of this ion is in good agreement with the observations from the charge-exchange experiments. A full analysis of the potential energy surface suggests that, at low ionizing energies ($\leq$11.5 eV), essentially all of the long-lived molecular ions have isomerized to **2**. The present example reveals the versatility and some of the advantages of the high-temperature near-blackbody-induced dissociation (hot wire emission) for probing structural problems in ion chemistry.

Introduction

Photodissociation of gas-phase ions driven by sequential absorption of infrared photons was pioneered by Beauchamp and co-workers about 25 years ago.[1] Since then, the use of low-power cw CO_2 lasers to promote multiphoton excitation and dissociation of trapped ions has become well-established as a useful tool in gas-phase ion chemistry and mass spectrometry.[2] Important applications have emerged from this type of infrared photodissociation, such as infrared spectroscopy of ions,[3] differentiation of isomeric ion structures,[4] biomolecule sequencing,[5] and determination of activation energies from photofragmentation rate constants measured as a function of laser intensity.[6]

A second approach for slow activation, and dissociation, of gas-phase ions has been the use of near-ambient-temperature blackbody radiation.[7] By studying the temperature dependence of the dissociation process, this method has proven to be particularly attractive for deriving activation energies and bond dissociation energies of ions.[8] Several examples have been illustrated in recent years both for relatively simple ions[9] and for ions of biochemical relevance.[10] Blackbody-induced dissociation has also been helpful in probing the structure of large cluster ions[11] and in possible sequencing of biomolecules.[12]

In recent years, we have explored an alternative method of infrared multiphoton activation of ions that combines some of the features of the CO_2 laser and of the ambient-temperature blackbody radiation experiments.[13−17] In our case, a heated wire acting as a high-temperature near-blackbody source (sometimes referred to as a graybody) is placed in close proximity to the cell of an FT-ICR spectrometer and provides considerable IR radiation in the important 1500−4000 cm^{-1} range. As in the CO_2 laser experiment, ions reach an effective internal temperature[18] that is lower than the radiation temperature but dependent on the position of the heated wire and the geometric parameters of the cell. This arrangement has two distinct advantages: (i) dissociation rates are much higher than those observed in near-room-temperature blackbody radiation experiments because of the higher internal temperature of the ions, and (ii) the internal temperature of the ions can be varied by changing the temperature of the heated wire, thus avoiding the difficult task of working with a homogeneously heated vacuum system in an FT-ICR spectrometer. In the most extensive study, we have shown that activation energies obtained from measuring dissociation rate constants at different radiation temperatures could be used to extract the dissociation energy of the molecular ion of acetophenone by a master equation approach.[14] (See Scheme 1).

SCHEME 1

$$C_6H_5COCH_3^{+\cdot} \rightarrow C_6H_5CO^+ + {}^{\cdot}CH_3$$

$$Do = 82.0 \pm 2.1 \text{ kJ mol}^{-1}$$

These experiments also proved to be a powerful method for distinguishing between the keto and enol tautomers of the molecular ion because the latter ion undergoes proton transfer to the neutral substrate much more rapidly than thermal dissociation at pressures in the 10^{-8} Torr.[16,19]

An extension of our studies to substituted acetophenones reveals that this “graybody dissociation”[17] method can be a

---

[†] Part of the special issue “Jack Beauchamp Festschrift”.

* Address for correspondence: Instituto de Química, University of São Paulo, Caixa Postal 26077, São Paulo, Brazil, CEP 05513-970. Phone/Fax: 55-11-3091-3888. E-mail: jmrnigra@iq.usp.br.

10.1021/jp0205923 CCC: $22.00

SCHEME 2

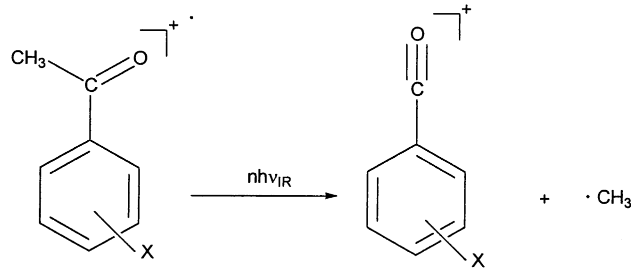

SCHEME 3

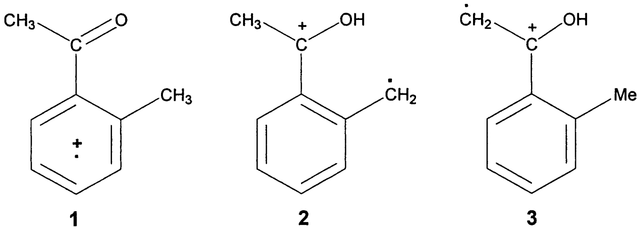

robust technique for some applications. The results reported in this paper reveal the following: (a) The temperature dependence of the dissociation rate constants induced by our high-temperature near-blackbody radiation source are similar (as would be expected) for a number of substituted acetophenones. (For example, see Scheme 2). This methyl-cleavage process is the main primary fragmentation process in these aromatic ketones, and its identification was established in the early years of organic mass spectrometry.[20] (b) A much higher apparent activation energy is obtained for the case of the molecular ion 2′-methylacetophenone. This latter result combined with ab initio calculations strongly indicates that the original molecular ion isomerizes completely to an enol structure generated by migration of a hydrogen from the ortho methyl group and that, in fact, three different isomers play an important role in the overall ion chemistry (Scheme 3).

Methods

Experimental Techniques. Experiments were carried out in an FT-ICR spectrometer of in-house design that operates typically at a magnetic field of 1 T supplied by an electromagnet. The general features of the spectrometer and the basic experimental procedure for the present work have been described in recent related publications from this group.[14,16,21] Ions were generated directly in the 15.6-cm^3 cubic cell by electron ionization in two different ways: (a) by applying a 40-ms pulse on the voltage of the rhenium filament from +10 V to the ionizing energy chosen for the particular experiment or (b) by pulsing the current on the ionization filament for a typical duration of 400 ms. This latter mode of operation is essential for detailed studies of the dissociation process under the influence of our independently heated wire because the light emitted by the ionizing filament in procedure a can promote the complete dissociation of the molecular ion of most of the substituted acetophenones in less than 3 s. Thus, method a was used only for qualitative studies related to thermal dissociation or ion/molecule reactions.

Studies of the dissociation of molecular ions induced by thermal radiation were carried out using a heated tungsten ribbon (0.0025 cm × 0.076 cm, W340, Scientific Instruments Services) mounted outside the ICR cell about 0.5 cm from one of the receiver plates. A rectangular opening in this plate allows the ions to be exposed to the radiation emitted by the tungsten wire. The heating of this tungsten ribbon is controlled by a Hewlett-Packard 6621A power supply, and the radiation temperature (typically in the 650−1400 K range) is determined as before.[14]

Molecular ions of the substituted acetophenones, $M^{+\bullet}$, were isolated at variable times after ion formation by ejection of the fragment ions with radio frequency pulses. On the other hand, the $(M + 1)^+$ ions, a mixture of the protonated substituted acetophenone and ^{13}C-containing molecular ions, were not ejected to avoid any undesirable excitation of the $M^{+\bullet}$ ions. Thus, the kinetics recorded for the $(M + 1)^+$ ions reflect a competition between thermally induced dissociation of the ^{13}C molecular ion and formation of the protonated species by ion/molecule reactions.

The reagents used in this work, namely, 2′-chloroacetophenone, 2′-methylacetophenone, 3′-methylacetophenone, 4′-methylacetophenone, 2-ethoxyethanol, and ferrocene, were obtained from Aldrich and subjected to freeze, pump, and thaw cycles prior to introduction into the high-vacuum system of the spectrometer. Other reagents are similar to those used in ref 16. Methyl disulfide was kindly provided by Prof. Liliana Marzorati of the Instituto de Química, Universidade de São Paulo.

A grating tunable cw CO_2 laser (SYNRAD, model 48G-1) was used for the infrared laser dissociation experiments. The laser was operated on the 976.6 cm^{-1} line, and no attempt was made to investigate the full wavelength dependence of the dissociation processes. The power level of the laser was externally controlled by varying the width of a 10-kHz modulation pulse provided by a Hewlett-Packard pulse generator. The laser power measured at the exit window of the vacuum system of the spectrometer was ∼1 W. The irradiation time was controlled by electronically varying the duration of the open time of a Uniblitz shutter placed in front of the laser. As previously mentioned,[21c] the water cooling and room temperature were maintained below 20 °C to minimize power fluctuations of the laser output.

Pressure was measured with an ion gauge located between the cell and the turbomolecular pump of the high-vacuum system of the spectrometer. The thermal dissociation experiments were carried out typically at nominal pressures in the $(0.5-2) \times 10^{-8}$ Torr range.

Ab Initio Calculations. Calculations to supplement the experimental observations were carried out with the Gaussian 98 suite of programs[22] running on a PC/Pentium II 450-MHz computer using the Linux operating system.

Structures were optimized at the HF/6-31G(d) level, and final energies were calculated at the MP2/6-31G(d) level. For the radical cations and the methyl radical, geometry optimization was carried out at the ROHF/6-31G(d) level, and energies were computed at the ROMP2/6-31G(d) level. A scaling factor of 0.89 was used for the zero-point energies (ZPE) in all final energy calculations. Stable stationary points were confirmed by frequency analysis, and transition states were characterized by one imaginary frequency. The fact that optimized transition states correspond to the desired transition states was confirmed by verifying the atom displacements associated with the normal mode of the imaginary frequency.

Results and Discussion

The mass spectra of the different methylacetophenone isomers obtained by electron ionization at 12 eV are very similar and are characterized by prominent peaks due to the $(M - 15)^+$ (*m*/*z* 119) fragment and the molecular ion $M^{+\bullet}$ (*m*/*z* 134).[23] At these low energies, the only significant other fragment ion,

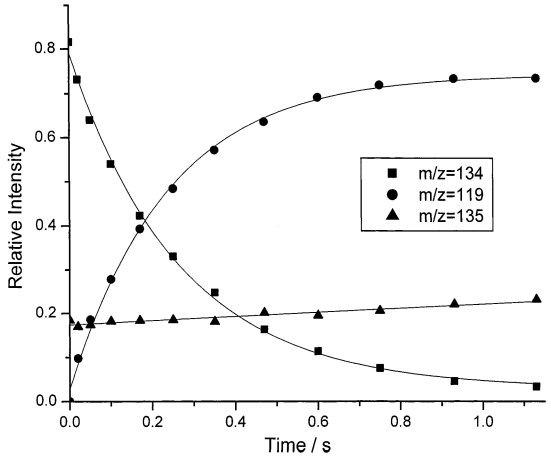

Figure 1. Kinetics of the disappearance of the molecular ion of 3′-methylacetophenone generated at 11.5 eV with the heated wire at an effective blackbody radiation temperature of $T = 1024$ K at a pressure of 8×10^{-9} Torr. The $(M + 1)^+$ ion represents the sum of the ^{13}C molecular ion and protonated 3′-methylacetophenone.

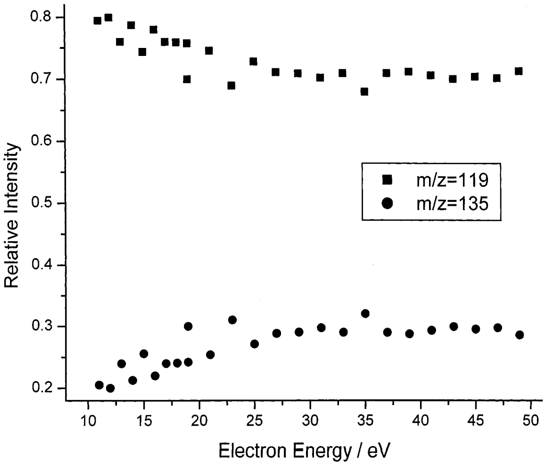

Figure 2. Relative intensities of the $(M - 15)^+$ (m/z =119) and $(M + 1)^+$ (m/z = 135) measured after all of the molecular ions of 3′-methylacetophenone have reacted by thermal dissociation and proton transfer at a nominal pressure of 7.5×10^{-9} Torr.

SCHEME 4

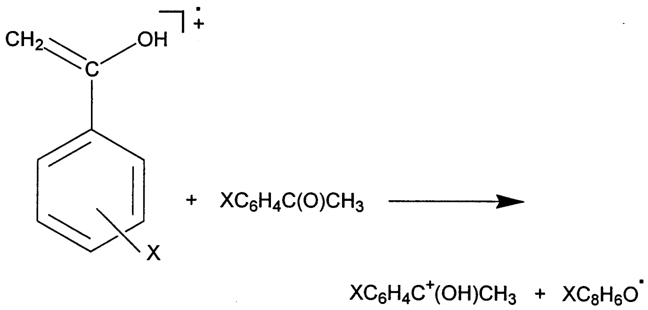

$(M - 43)^+$ (m/z 77), amounts to less than 9%. The IEs reported from this early study reveal the trend IE(para) 9.17 ± 0.02 eV < IE(meta) 9.24 ± 0.02 eV ≤ IE(ortho) 9.27 ± 0.01 eV, but the absolute values must be viewed with caution. These values are just below the accepted value of 9.28 eV for acetophenone obtained by photoionization techniques.[24] A photoelectron study[25] of 2′-methylacetophenone reported a somewhat lower ionization energy, but more important, it revealed three bands originating from a symmetric ring π orbital (9.15 eV), from the n orbital on O (9.32 eV), and from an antisymmetric π orbital (9.44 eV). Although similar studies are not available for the other isomers, the lowest IE should also correspond to removal from a symmetric ring π orbital.

1. Thermally Induced Dissociation of Substituted Acetophenones. Figure 1 shows the kinetic behavior of isolated molecular ions of 3′-methylacetophenone, m/z 134, generated by the pulsed-current electron ionization method at 11.5 eV and under the influence of the radiation emitted by the heated tungsten wire. Thermally induced dissociation of the molecular ion resulting in loss of a methyl group (Scheme 2) is clearly the most significant process. As in our previous experiments with acetophenone,[14,16] formation of the protonated form, m/z 135, through ion/molecule reactions of the molecular ion with its neutral precursor is a minor channel at the pressures used in our experiments and at low electron energies (≤13 eV). At higher electron energies, the contribution of the bimolecular channel(s) responsible for formation of the m/z 135 ion increases significantly (see Figure 2).

The above observations are consistent with the fact that the proton transfer reaction is promoted by the enol form of the molecular ion (**3**) as was previously found for acetophenone and some of the fluorine-substituted acetophenones.[16]

The enol species in acetophenones is formed predominantly through a tautomerization process involving a double 1,4-hydrogen migration:[16] transfer of an ortho ring hydrogen to the carbonyl oxygen followed by transfer of a methyl hydrogen to the ring. Although enol isomers of ketone radical cations are known to be more stable than the keto isomer,[26] a substantial barrier exists for this tautomerization,[16] and thus formation of the enol isomer is expected to become more favorable at higher ionizing energies where more internal energy can be deposited in the nascent molecular ion. A second pathway for enol formation in acetophenone has also been invoked and involves a catalyzed bimolecular isomerization resulting in 1,3-hydrogen migration from the carbonyl methyl group.[27] The proton-transfer reaction shown in Scheme 4 is highly favored because of the high proton affinity of the substituted acetophenones.[28]

The behavior of the molecular ions of 2′-chloroacetophenone and 4′-methylacetophenone is very similar to that displayed in Figures 1 and 2. The only significant difference was observed for 4′-methylacetophenone at the lowest radiation temperatures used in this work (~700 K) where dissociation becomes very slow after ~3 s.

A dramatic difference occurs under similar conditions for the molecular ion of 2′-methylacetophenone (see Figure 3). At a similar radiation temperature of the heated tungsten wire, the observed dissociation rate constant for the molecular ion of 2′-methylacetophenone is about 57 times smaller than that of the molecular ion of 3′-methylacetophenone.

Differences in the dissociation rate constant are also observed in the cw CO_2 laser-induced-dissociation experiments. In Figure 4, we compare the dissociation rate for the molecular ions of 2′- and 3′-methylacetophenone, produced by the pulsed electron energy method, and thus exposed to the radiation of the ionization filament, with and without irradiation of the CO_2 laser as described in the Experimental Section. It is clear that the ionization filament is quite effective as a source of IR radiation to promote the dissociation of the 3′-methylacetophenone radical cation but not that of the 2′-methylacetophenone. In the latter case, the CO_2 laser has a pronounced effect on the dissociation rate.

A more revealing result about the ease of thermal dissociation among the substituted acetophenones can be obtained by varying the temperature of the radiation source. In our previous work,[14]

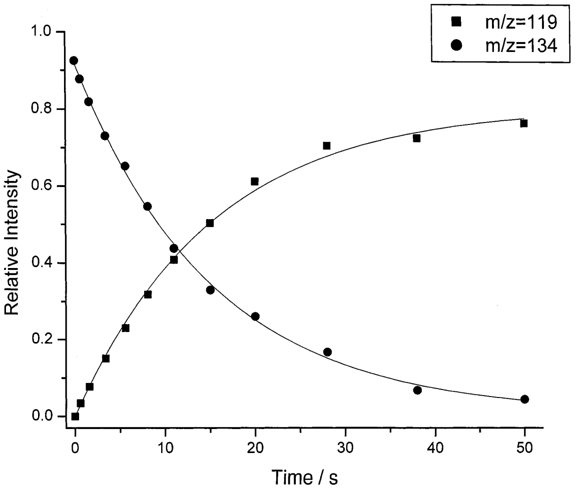

Figure 3. Kinetics of the disappearance of the molecular ion of 2′-methylacetophenone generated at 11.5 eV with the heated wire at an effective blackbody radiation temperature of $T = 1046$ K at a pressure of 1×10^{-8} Torr. This graph does not include the kinetic behavior of the $(M + 1)^+$ ion (the sum of the ^{13}C molecular ion and protonated 2′-methylacetophenone), but its intensity is computed in calculating the relative intensities.

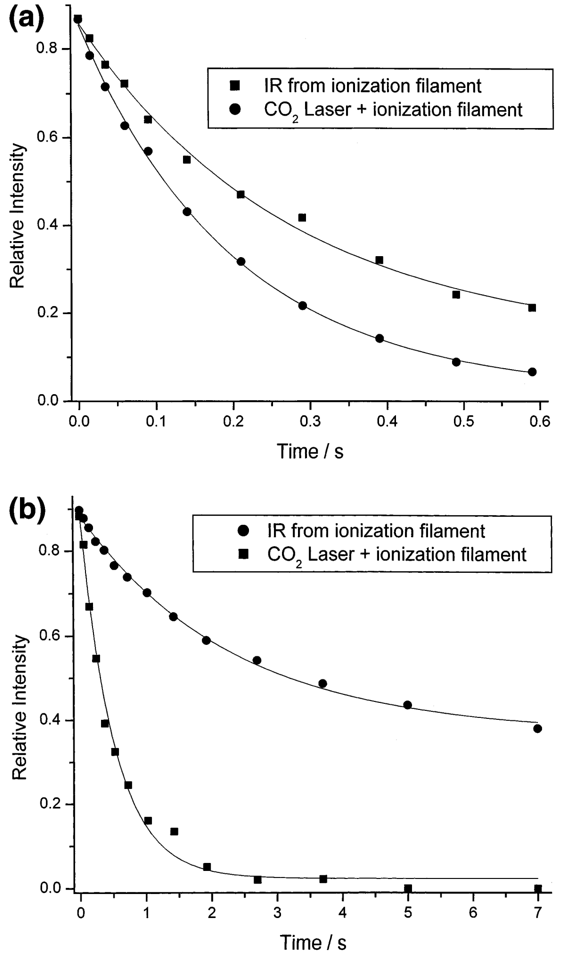

Figure 4. Dissociation kinetics induced by the combined effects of the light emitted by the ionization filament and a cw CO_2 laser: (a) 3′-methylacetophenone molecular ion, (b) 2′-methylacetophenone.

it was shown that the hot tungsten wire can be treated as an approximate blackbody provided that the radiance is corrected to that of an equivalent blackbody temperature. This correction entails a well-known conversion of the radiation emitted by tungsten at a certain temperature (T) to the equivalent integrated radiation emitted by a blackbody at temperature T_b. Furthermore, master equation simulations[17,18,29] show that, under certain conditions, Arrhenius-type plots can be constructed for the dissociation rate constants as a function of the effective blackbody radiation temperature to obtain activation energies. Although a full treatment of how to obtain reliable activation energies was not pursued in the present case, Figure 5 displays for comparison the variation of the overall reaction rate constants (unimolecular and bimolecular) for a number of substituted acetophenones as a function of T_b using acetophenone as a standard.[30] The slopes of these Arrhenius-type plots obtained for the 3′- and 4′-methylacetophenone molecular ions agree to within 10% (essentially to within the experimental error of the fit) with that of the acetophenone molecular ion, indicating that the activation energies for dissociation of these three molecular ions are very similar as might be expected. On the other hand, the slope of the Arrhenius-type plot for the molecular ion of 2′-methylacetophenone is 2.1 ± 0.2 larger than that of the acetophenone ion, clearly indicating that a much higher activation energy is present for dissociation of the 2′-methylacetophenone molecular ion. By comparison, we are led to conclude that the activation energy for dissociation of the 2′-chloroacetophenone molecular ion is somewhat lower than that of acetophenone.

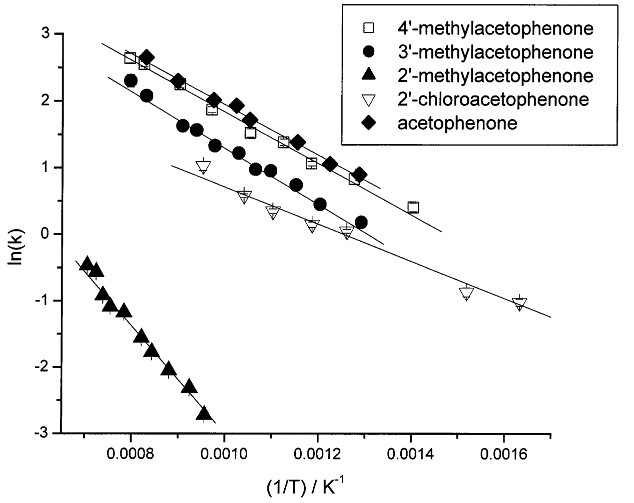

Figure 5. Arrhenius-type plots for the overall reaction rate constant of the molecular ions of substituted acetophenones compared with that of acetophenone.

These results clearly show that the 2′-methylacetophenone molecular ion represents an anomaly because it dissociates more slowly than the other acetophenones. Previous work on the metastable transitions involving cleavage of the carbonyl methyl group from the molecular ions of the isomeric methylacetophenones (a chemical process similar to that shown in Scheme 2) reveals that the ortho isomer exhibits a slightly higher kinetic energy release (KER) than the other isomers.[31] Although the measured KER is not clearly indicative of a reverse activation energy for the dissociation process, this early study raised the possible contribution of the enol structure **2** for the 2′-methylacetophenone radical cation originating from a facile hydrogen migration of the ring methyl group to the carbonyl oxygen. This particular type of keto−enol isomerization is well-known for neutral 2′-methylacetophenone, where photoenolization of the keto species proceeds via a biradical triplet state, with the less stable enol form returning to the keto form through a thermal process.[32]

Conclusive evidence about the enol radical cation **2** has been obtained from radiolytic ionization of 2′-methylacetophenone

SCHEME 5

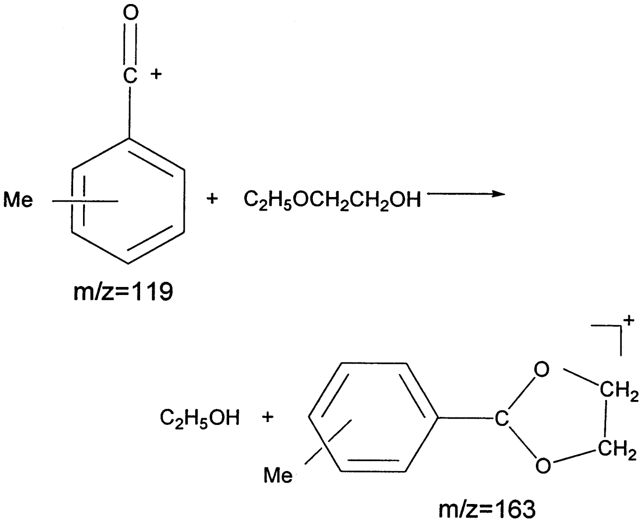

SCHEME 6

$$\mathrm{PhC(OH)CH_2^{+\cdot} + CH_2{=}CHMe \rightarrow C_{11}H_{12}^{+} + H_2O}$$

in low-temperature matrixes,[33] and the activation energy for the unimolecular tautomerization of **1** to **2** was determined to be only 12.5 kJ mol^{-1} at 90 K. This enol form then raises the question as to whether cleavage of the methyl group entails a different mechanism characteristic of ortho effects in mass spectrometry.[34,35]

2. Chemical Probes of the Fragment and Molecular Ions of the Methylacetophenones. On the basis of the experimental results obtained for the 2′-methylacetophenone molecular ion, we decided to explore other methods of characterizing both the fragment ion produced in the dissociation and the molecular ion undergoing dissociation.

For the case of the fragment ion, a diagnostic ion/molecule reaction has recently been proposed to be specific for recognizing acylium ions.[36,37] For example, acylium ions are expected to undergo readily a ketalization reaction with substrates such as ethoxyethanol (see Scheme 5).

This reactivity was then used to probe whether the fragment ions do, in fact, correspond to benzoyl ions. The *m*/*z* 119 fragment ions obtained directly following electron ionization and those resulting from thermally induced dissociation of the molecular ion were investigated in this fashion. In the first case, fragment ions were typically isolated 200 ms after ionization and allowed to react with ethoxyethanol. The $C_8H_7O^+$ fragment ions from all three methylacetophenone isomers readily yield the *m*/*z* 163 product ions. In the second case, *m*/*z* 119 fragment ions obtained from the thermally induced dissociation of the molecular ions were typically isolated after one half-life of the dissociation process. As in the former case, ions obtained in this way from all three isomers react readily according to Scheme 5. These results are indicative that, in all cases, including 2′-methylacetophenone, the fragment *m*/*z* 119 can be characterized as an acylium ion, as shown in Scheme 5.

A second set of experiments was performed to establish the identity of the molecular ions. Our first attempt was to establish the presence of enol-type ions in the different isomers of methylacetophenone by reaction with an alkene such as propene. It has been shown that phenyl-substituted enol radical cations undergo addition of an alkene followed by elimination of water to yield presumably a cyclic ion.[38,39](See Scheme 6).

SCHEME 7

$$m\text{- or }p\text{- }\mathrm{MePhC(O)CH_3^{+\cdot} + MeSSMe \rightarrow}$$
$$m\text{- or }p\text{- }\mathrm{MePhC(O)CH_3 + MeSSMe^{+\cdot}}$$

We were unsuccessful in observing this reaction for $M^{+\bullet}$ ions originating from any of the methylacetophenone isomers. However, a dramatic increase is observed in the formation of the $(M + 1)^+$ ions, indicating that presumably enol ions are formed bimolecularly and transfer proton rapidly to the parent methylacetophenone.

A second set of experiments was carried out with dimethyl disulfide, MeSSMe, a well-known reagent for distonic ions.[40] Unlike other distonic ions that abstract MeS•· from dimethyl disulfide, enol distonic ions usually react by electron transfer similarly to the keto isomer.

The molecular ions of 3′- and 4′-methylacetophenone, most of them presumably in their keto form in our experiments, undergo fast charge-transfer reactions with MeSSMe as shown in Scheme 7.

This is consistent with the fact that the IE of MeSSMe is considerably lower than that of the acetophenones.[41] By comparison, no more than 10% of slow charge transfer is observed from the $M^{+\bullet}$ ion of 2′-methylacetophenone. This is highly indicative that the recombination energy of the 2′-methylacetophenone $M^{+\bullet}$ ion is *less* than the ionization energy of MeSSMe.

Given the present uncertainty in the value of the IE for MeSSMe (see ref 41), additional experiments were carried out with ferrocene, $Fe(C_5H_5)_2$, for which ionization energy values of 6.82 eV from charge-exchange equilibrium experiments by FT-ICR spectroscopy[42] and 6.747 ± 0.009 eV from photoionization experiments have been obtained.[43] Experiments carried out with ferrocene in our spectrometer reveal that the 2′-methylacetophenone $M^{+\bullet}$ ions undergo a charge-transfer reaction until completion although the reaction is not fast. This experiment suggests that the recombination energy of the 2′-methylacetophenone $M^{+\bullet}$ ion is probably comparable to the IE of ferrrocene and is a strong indication that these ions do not retain their keto structure.

Further insight into this problem can be gained from the results obtained from the ab initio calculations presented and discussed below.

3. Results of the ab Initio Calculations. The geometries for neutral molecules and ions were optimized at the HF/6-31G(d) level for closed-shell species and at the ROHF/6-31G(d) level for open-shell species as outlined in the Methods section.[44] Neutral acetophenones were found to have a plane of symmetry with all of the heavy atoms on the plane, whereas in the keto and enol molecular ions, there is a departure from this planar arrangement. The only exception is the enol species **2**, in which all heavy atoms lie in a plane of symmetry.

Vibrational frequencies were also calculated for these structures at this level of theory and the unscaled zero-point energies are listed in Table 1 for the most relevant species. For comparison purposes, we also carried out a similar calculation for acetophenone for which the experimental[45] ZPE amounts to 350 kJ mol^{-1}. The calculated unscaled ZPE at the HF/6-31G(d) level corresponds to 383.4 kJ mol^{-1}, which, when scaled by 0.89, leads to an error of 9 kJ mol^{-1}. Thus, relative errors in ZPE can give rise to additional uncertainties in the final calculated molecular energies.

The electronic energies for these structures were then calculated at the MP2/6-31G(d) level for closed-shell species

TABLE 1: Calculated Energies (in au) at the ROMP2/6-31G(d)//ROHF/6-31G(d) Level for Open-Shell Species and at the MP2/6-31G(d)//HF/6-31G(d) Level for Closed-Shell Species

molecule	ion	E_{elet}	ZPE[a]
CH_3		−39.668 177 0	82.00
2′-$ClC_6H_4COCH_3$	keto	−842.361 296 6	358.17
	enol	−842.363 476 8	361.36
2′-ClC_6H_4CO	2′-$ClC_6H_4CO^+$	−802.653 751 8	252.82
4′-$CH_3C_6H_4COCH_3$	keto	−422.512 254 0	460.74
	enol	−422.518 885 3	463.59
4′-$CH_3C_6H_4CO$	4′-$CH_3C_6H_4CO^+$	−382.805 819 4	356.12
3′-$CH_3C_6H_4COCH_3$	keto	−422.514 601 6	461.19
	enol	−422.516 741 4	464.36
3′-$CH_3C_6H_4CO$	3′-$CH_3C_6H_4CO^+$	−382.804 227 3	356.60
2′-$CH_3C_6H_4COCH_3$	**1**	−422.510 265 2	462.17
	2	−422.517 378 8	465.58
	3	−422.511 459 9	466.13
2′-$CH_3C_6H_4CO$	2′-$CH_3C_6H_4CO^+$	−382.805 213 8	356.16

[a] Unscaled ZPEs in kJ mol^{-1}.

TABLE 2: Dissociation Energies Calculated for the Keto Isomer of the Molecular Ions in Scheme 2[a,b]

	E_{elet} (au) keto $[M]^{+\bullet}$	E_{elet} (au) $F^+ + Me^\bullet$	ΔZPE (kJ mol^{-1})	E_{diss} (kJ mol^{-1})
2′-chloroacetophenone	−842.361 296 6	−842.321 928 8	−23.35	82.6
4′-methylacetopenone	−422.512 254 0	−422.473 996 4	−22.62	80.3
3′-methylacetopenone	−422.514 601 6	−422.472 404 3	−22.59	90.7
2′-methylacetopenone	−422.510 271 7	−382.805 211 0	−24.01	75.4

[a] Tabulated ΔZPEs are unscaled. [b] Tabulated E_{diss} values include ΔZPE corrections scaled by a factor of 0.89.

TABLE 3: Stabilization Energies for the Enol Molecular Ions[a]

	$(E_{\text{enol}} - E_{\text{keto}})$ (kJ mol^{-1})
2′-chloroacetophenone	−2.9
4′-methylacetophenone	−14.9
3′-methylacetophenone	−2.8
2′-methylacetophenone	−0.4 (enol 3)
	−15.6 (enol 2)

[a] Values include ZPE corrections scaled by 0.89.

or at the ROMP2/6-31G(d) level for open-shell species, and the values are listed in Table 1.

Table 2 lists the calculated dissociation energies (Scheme 2) for the four substituted acetophenones discussed in the present work. For the sake of comparison, dissociation energies were computed for the keto radical cation. Considering that the level of calculation can probably estimate reaction energies within 15 kJ mol^{-1}, no significant differences are observed except for the fact that for the 3′-methylacetophenone the calculated dissociation energy seems to be somewhat higher. These calculated values are within the range of dissociation energy of 82 kJ mol^{-1} determined in our previous work for the molecular ion of acetophenone.[14]

A second important consideration concerns the relative stabilities of the different keto and enol ions of the methylacetophenones. These relative energies are listed in Table 3. It is noticeable that the $XC_6H_4C(OH)CH_2^{+\bullet}$ enol species are generally somewhat more stable than the corresponding $XC_6H_4C(O)CH_3^{+\bullet}$ keto species but the differences in stability are much less than the 50−60 kJ mol^{-1} found in aliphatic ketones[26] and 80−120 kJ mol^{-1} found in esters.[46,47] This is likely because the lowest electronic state of the keto acetophenone ions arises from the removal of a π electron from the ring and our calculations consistently predict this state to be the lowest electronic state.

SCHEME 8

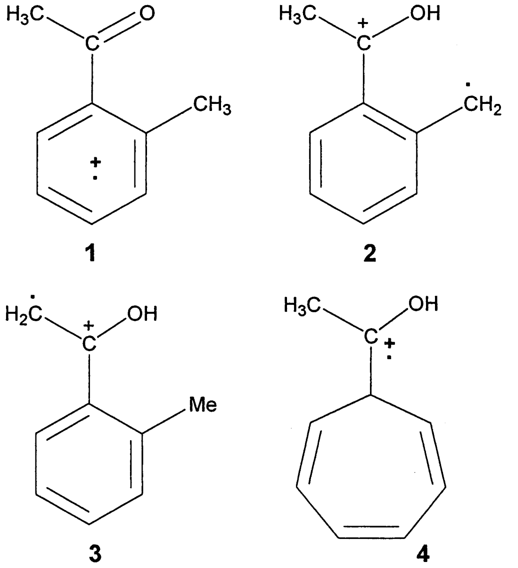

To understand the behavior of the 2′-methylacetophenone radical cation, a more extensive exploration of the potential energy surface was carried out to characterize possible isomeric species for the molecular ion, transition states for isomerization, and possible dissociation products.

Four possible isomers were considered for the 2′-methylacetophenone radical cation, (Scheme 8)

Calculations also included intermediate species involved in the tautomerization process and their respective transition states along with fragment ions originating from loss of a methyl group from the molecular ion. The stable species considered here are shown in Scheme 9.

Table 4 lists the calculated energies and ZPE's of the relevant species that have been used to construct the potential energy surface for the molecular ion of 2′-methylacetophenone. For example, only the most stable **2** *Z* isomer is shown, and the keto isomer of **4** has been omitted because it is calculated to be 109 kJ mol^{-1} higher in energy than **4**. The relative energy values are listed with and without corrections for zero-point energies (ZPE) because the MP2/6-31G(d)//HF/6-31G(d) level of calculation used in our work is probably not of sufficient accuracy for the size of these ions (also see below). It is clear that some significant changes are observed for these two criteria, particularly for the transition states and the dissociation channel.

Figure 6 is a graphic representation of the potential energy surface for the 2′-methylacetophenone radical cation (including ZPE corrections) resulting from our calculations. Although this energy surface is useful and essential to our discussion, it is important to emphasize that the relative values must be viewed with caution because all of the calculations are based on a single electronic configuration. Considering the fact that there are two close-lying excited electronic states for the radical cation,[26] a multiconfiguration approach might be necessary in this case to obtain more reliable energies.

Bearing in mind the possible limitations of a single-configuration approach, the first important observation is related to the products of dissociation. The calculated dissociation energy from the keto radical cation into a benzoyl cation and a methyl radical, 75.4 kJ mol^{-1} (ZPE corrected) and 96.8 kJ mol^{-1} (without ZPE corrections), is well below that of any other alternative. For example, using ion **1** as our reference (a) the dissociation energy for cleavage of the ortho methyl group to

SCHEME 9

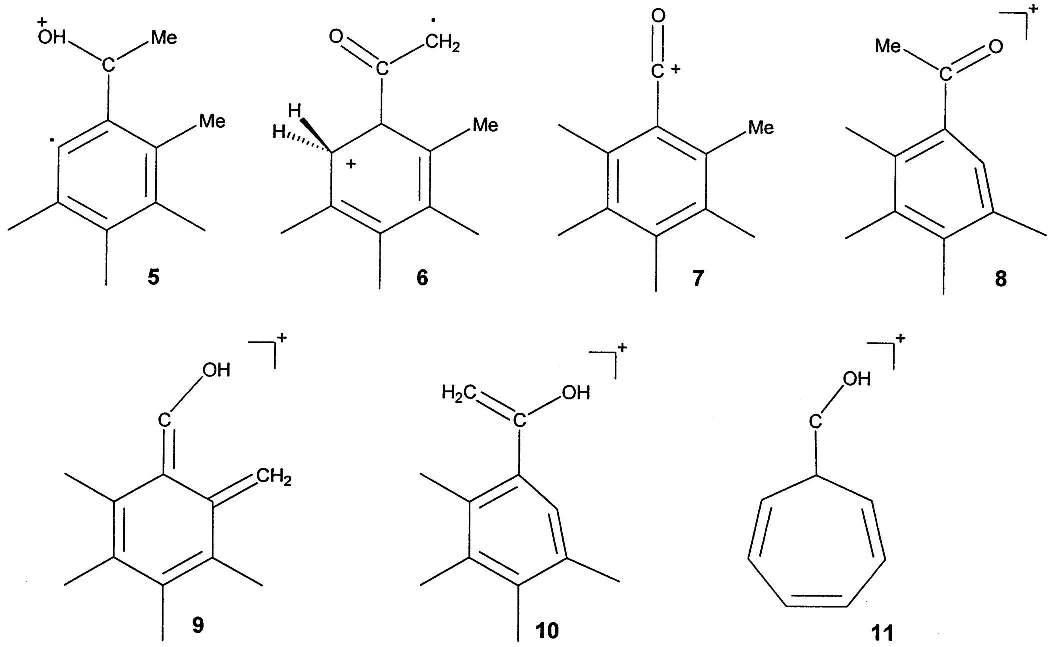

TABLE 4: Calculated Energies (in au) and Unscaled Zero-Point Energies, ZPEs (in kJ mol^{-1}), for the Relevant Species in the Potential Energy Surface Shown in Figure 6

	E_{elet}	$\Delta E = E_i - E_1$[a]	ZPE	$\Delta E + 0.89 \times \Delta\text{ZPE}$[b]
1	−422.510 265 2	0.0000	462.17	0.00
2	−422.517 378 8	−18.7	465.58	−15.6
TS1/2	−422.498 292 4	31.4	449.10	19.8
3	−422.511 459 9	−3.1	466.12	0.4
TS1/3	−422.450 377 5	157.2	450.16	146.5
TS2/3	−422.478 797 4	82.6	451.30	72.9
7 + Me	−382.805 213 8	96.8	356.16	75.4
5	−422.484 106 5	68.7	467.50	73.4
TS1/5	−422.462 977 4	124.2	448.50	112.0
TS5/3	−422.451 789 0	153.5	451.92	144.4
6	−422.465 964 9	116.3	456.65	111.4
TS1/6	−422.436 033 6	194.9	445.82	180.4
TS6/3	−422.454 991 4	145.1	447.29	131.9
4	−422.525 507 8	−40.0	472.41	−30.9

[a] Relative electronic energies with respect to species **1** used as the reference (in kJ mol^{-1}). [b] Relative electronic energies with respect to species **1** used as the reference, including the scaled values for zero-point energies, $\Delta\text{ZPE} = \text{ZPE}_i - \text{ZPE}_1$ (in kJ mol^{-1}).

yield ion **8** and Me• is calculated to be 413 kJ mol^{-1}, (b) the dissociation energy for cleavage of the methyl group to yield ion **9** and Me• is calculated to be 446 kJ mol^{-1}, (c) the dissociation energy for cleavage of the ortho methyl group to yield ion **10** and Me• is calculated to be 460 kJ mol^{-1}, and (d) the dissociation energy for cleavage of the methyl group to yield ion **11** and Me• is calculated to be 407 kJ mol^{-1}.

This theoretical prediction is in good agreement with the experimental results, which argue strongly for a benzoyl structure for the fragment ion originating in the dissociation process. As in most bond-cleavage processes, these calculated dissociation energies are considered to be relevant to the kinetic problem if a negligible reverse activation energy is assumed.

The potential energy surface shown in Figure 6 is also very enlightening considering the tautomerization pathways for species **1** to interconvert into the enol species **2** and **3**. The direct isomerization **1** → **3** by a 1,3-hydrogen migration is predicted to involve a high barrier (147 kJ mol^{-1}), in good agreement with what has been found in acetone.[48] On the other hand, the lowest pathway for this isomerization process is predicted to be similar to that found for the acetophenone radical cation,[16] namely, transfer of an ortho hydrogen to the oxygen by a 1,4-hydrogen migration to yield the stable distonic ion **5**, followed by a second 1,4-hydrogen migration from the methyl group to the ortho position. Nevertheless, it is disturbing to observe that even this pathway lies considerably above the dissociation energy. Because species **3** is predicted to be essentially isoenergetic with **1**, the slowness of the dissociation process observed in our experiments cannot be explained by assuming that dissociation occurs from **3**.

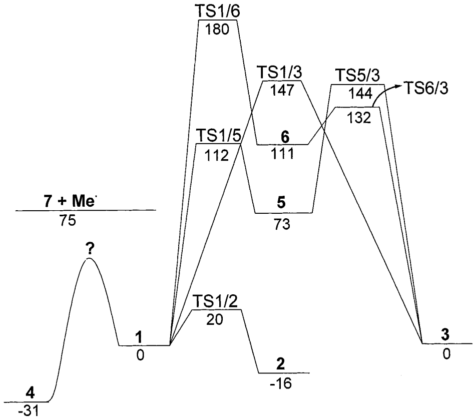

Figure 6. Calculated potential energy surface (including ZPE corrections) for isomerization and dissociation of the 2′-methylacetophenone molecular ion. Although not shown for the sake of clarity, **TS 2/3** is located 73 kJ mol^{-1} above **1**, and the lowest energy path for formation of **3** is thus **1** → **2** → **3**.

The most important result concerns the **1** → **2** tautomerization pathway. First, the enol form **2** is predicted to be more stable than **1**, but more important, this isomerization proceeds through a low-energy barrier (20 kJ mol^{-1}). Our calculated value is consistent with the 12.5 kJ mol^{-1} activation energy determined for this enolization process from low-temperature work.[33] Considering that the average vibrational internal energy of the **1** ions at 298 K is calculated to amount to 16.7 kJ mol^{-1} (obtained with unscaled frequencies), it is thus very likely that essentially all of the long-lived **1** ions isomerize to **2**. This

TABLE 5: Calculated Energies (in au), Unscaled Zero-Point Energies, ZPEs (in kJ mol^{-1}), and Calculated Ionization Energies (in eV) for the Relevant Species in the 2′-Methylacetophenone Molecular Ion System

	E_{elet}	IE[a]	ZPE	IE[b]
1	−422.510 265 2		462.17	
neutral **1**	−422.825 401 3	8.57	468.06	8.52
2	−422.517 378 8		465.58	
neutral **2**	−422.744 348 4	6.18	467.03	6.16
3	−422.511 459 9		466.12	
neutral **3**	−422.796 157 2	7.75	467.43	7.74
4	−422.525 507 8		472.41	
neutral **4**	−422.739 836 5	5.83	467.59	5.88
$MeSSMe^{+\bullet}$	−874.471 696 2		219.23	
MeSSMe	−874.752 741 6	7.65	219.43	7.65

[a] Ionization energies calculated without ZPE corrections. [b] Ionization energies including scaled ZPE corrections.

argument is further reinforced by the fact that, in this energy range, a tunneling mechanism might considerably enhance this tautomerization, as advocated for the reverse tautomerization process in neutral 2′-methylacetophenone.[49] These results would then predict that a substantially higher activation energy would be observed for the dissociation process **2** → **7** + $Me^{\bullet}$ and be in agreement with our experimental observations.

Although not shown in Figure 6 for the sake of clarity, we have also located the transition state connecting the two enol isomers (see Table 4). This transition state is located 72.9 kJ mol^{-1} (E_r + ZPE) above species **1**, used as our reference for the relative energy scale. Because this transition state is predicted to be below the energy for dissociation, the calculations suggest that the enol species **3** is actually formed via the **1** → **2** → **3** pathway. This pathway would then account for the small fraction of proton-transfer reaction observed and attributed to isomer **3**, a reaction that becomes more favorable when the molecular ion is generated with higher internal energy (see Figure 2).

One further process was considered as a potential isomerization pathway in this energy surface, which can be qualitatively described as a ring-expansion process of **2** to yield isomer **4**. Isomer **4** is by far the most stable species in this surface, lying 31 kJ mol^{-1} lower in energy than the keto molecular ion **1**. Although this is an interesting possibility, it was unclear to us as to whether the isomerization pathway leading to **4** involves passage through **2** and other intermediates or can proceed from **1** through a different pathway. Although transition states and intermediates were sought for these possibilities, we were unable to establish a mechanism for such a transformation. By way of comparison, it is important to remember that the molecular ion of toluene, $C_7H_8^{+\bullet}$ ($TOL^{+\bullet}$), is assumed to reach a dynamic equilibrium with the ring-expanded cycloheptatriene radical cation, $C_7H_8^{+\bullet}$ ($CHT^{+\bullet}$), prior to dissociation by hydrogen-bond cleavage to yield $C_7H_7^{+}$.[50] Although, in this case, the $CHT^{+\bullet}$ is considerably less stable than the $TOL^{+\bullet}$ cation, experimental and theoretical studies have placed the activation energy for this $TOL^{+\bullet} \rightarrow CHT^{+\bullet}$ process above 150 kJ mol^{-1}.[51] Thus, we are lead to believe that the **1** → ? → ? → **4** process probably does involve some high-energy pathway. This line of reasoning is supported by the failure to observe such a species in the tautomerization study carried out in matrixes at low temperatures.[33]

Finally, calculations directed toward understanding the electron-transfer reactions studied in this work provide further support to our conclusions. Table 5 lists the energies calculated for ions **1**−**4** along with their corresponding neutrals and for the dimethyl disulfide molecular ion and neutral used in the charge-exchange experiments, as well as the resulting energies of ionization (IE). The result of 7.65 eV obtained for dimethyl disulfide falls between the photoionization value (8.18 eV) and the value presently recommended in the NIST tables (7.4 eV).[41] By comparison, the IE obtained for 2′-methylacetophenone to yield **1** predicts an adiabatic ionization energy about 0.5 eV below the experimental value.[23,26] A similar result is obtained for the 3′- and 4′-methylacetophenones. Thus, it is apparent that our calculations underestimate the IE when compared with the experimental values.

The calculated ionization energies displayed in Table 5 are particularly significant regarding our arguments about isomers **2**−**4**. In fact, the recombination energies of both **2** and **4** are significantly lower than the calculated ionization energy of MeSSMe, whereas that of **3** is estimated to be slightly above that of dimethyl disulfide. On the other hand, bearing in mind that our IEs are underestimated, the value obtained for the recombination energy of **2** is consistent with the fact that significant albeit slow charge transfer occurs with ferrocene. This argument is considerably less favorable for **4** for which a substantially lower recombination energy is estimated that is almost 0.8 eV below the IE of ferrocene. These values again strongly support the idea that almost complete isomerization has occurred to the **2** ion.

Conclusions

The thermal dissociation of the 2′-methylacetophenone molecular ion induced by the near-blackbody radiation of a heated wire shows that the methyl-cleavage process is characterized by a much higher dissociation energy than that observed for other substituted acetophenones. Charge-exchange experiments clearly establish that this molecular ion does not retain the keto structure, as the recombination energy for this ion is much less than those observed for typical keto-like acetophenone ions.

The present experiments when coupled with ab initio calculations clearly point out that, on the time scale typical of FT-ICR techniques, the long-lived molecular ions have almost completely isomerized to the **2** ion through a low-barrier 1,4-hydrogen migration from the ring methyl group. They also show that the dissociation results from cleavage of the methyl group originally attached to the carbonyl group. Furthermore, the resulting fragment ion has been characterized as retaining a benzoyl structure.

The present dissociation process induced by slow pumping with polychromatic infrared radiation is an interesting case where excitation of **2** through its vibrational manifold presumably proceeds initially by absorption through its different vibrational modes. However, at excitation levels above the **2** → **1** barrier (estimated by our calculations to be 36 kJ mol^{-1}), both tautomers become indistinguishable and dissociation proceeds through the lowest-energy channel of the system.

Finally, this case provides an excellent example of the usefulness of the “hot wire” technique for promoting the dissociation of molecular ions in the cell of an FT-ICR spectrometer and for probing the structures of molecular ions.

Acknowledgment. This work was supported by the São Paulo Science Foundation (FAPESP) through a research grant and a Master’s degree fellowship (T.G.). We are particularly indebted to Dr. Josefredo Pliego Jr. for his help with the theoretical calculations and to Jair J. Menegon for his invaluable assistance with many of the experimental setups. One of us (J.M.R.) also acknowledges support of the Brazilian Research Council through its Senior Research Fellowship program. This work is dedicated to Jack Beauchamp on his 60th birthday for his many original, significant, and timely contributions to chemistry.

References and Notes

(1) (a) Bomse, D. S.; Woodin, R. L.; Beauchamp, J. L. *J. Am. Chem. Soc.* **1979**, *101*, 5503−5512. (b) Bomse, D. S.; Woodin, R. L.; Beauchamp, J. L. *J. Am. Chem. Soc.* **1979**, *101*, 5503. (c) Woodin, R. L.; Bomse, D. S.; Beauchamp, J. L. In *Chemical and Biochemical Application of Lasers*; Moore, C. B., Ed., Academic Press: New York, 1979; Vol. IV, pp 355−388. (d) Thorne, L. R.; Beauchamp, J. L. In *Gas-Phase Ion Chemistry*; Bowers, M. T., Ed.; Academic Press: New York, 1984; Vol. 3, pp 42−97.

(2) McLuckey, S. A.; Goeringer, D. E. *J. Mass Spectrom.* **1997**, *32*, 461.

(3) (a) Shin, S. K. S.; Beauchamp, J. L. *J. Am. Chem. Soc.* **1990**, *112*, 2066. (b) Peiris, D. M.; Riveros, J. M.; Eyler, J. R. *Int. J. Mass Spectrom. Ion Processes* **1996**, *156*, 169.

(4) (a) Baykut, G.; Watson, C. H.; Weller, R. R.; Eyler, J. R. *J. Am. Chem. Soc.* **1985**, *107*, 8036. (b) Gaumann, T.; Zhu, Z.; Kida, M. C.; Riveros, J. M. *J. Am. Soc. Mass Spectrom.* **1991**, *2*, 372.

(5) Little, D. P.; Speir, J. P.; Senko, M. W.; O'Connor, P. B.; McLafferty, F. W. *Anal. Chem.* **1994**, *66*, 2809.

(6) (a) Dunbar, R. C. *J. Chem. Phys.* **1991**, *95*, 2537. (b) Uechi, G. T.; Dunbar, R. C. *J. Chem. Phys.* **1992**, *96*, 8897. (c) Freitas, M. A.; Hendrikson, C. L.; Marshall, A. G. *J. Am. Chem. Soc.* **2000**, *122*, 7768. (d) Jockusch, R. A.; Paech, K.; Williams, E. R. *J. Phys. Chem. A* **2000**, *104*, 3188.

(7) (a) Thölmann, D.; Tonner, D. S.; McMahon, T. B. *J. Phys. Chem.* **1994**, *98*, 2002. (b) Price, W. D.; Schnier, P. D.; Williams, E. R. *Anal. Chem.* **1996**, *68*, 859.

(8) (a) Dunbar, R. C. *J. Phys. Chem.* **1994**, *98*, 8705. (b) Dunbar, R. C.; McMahon, T. B. *Science* **1998**, *279*, 194.

(9) See, for example: (a) Lin, C.-Y.; Dunbar, R. C. *J. Phys. Chem.* **1996**, *100*, 655. (b) Lin, C.-Y.; Dunbar, R. C.; Haynes, C. L.; Armentrout, P. B.; Tonner, D. S.; McMahon, T. B. *J. Phys. Chem.* **1996**, *100*, 19659. (c) Rodriguez-Cruz, S. R.; Jockusch, R. A.; Williams, E. R. *J. Am. Chem. Soc.* **1998**, *120*, 5842.

(10) See, for example: (a) Strittmatter, E. F.; Schnier, P. D.; Klassen, J. S.; Williams, E. R. *J. Am. Soc. Mass Spectrom.* **1999**, *10*, 1095. (b) Schnier, P. D.; Klassen, J. S.; Strittmatter, E. F.; Williams, E. R *J. Am. Chem. Soc.* **1998**, *120*, 9605. (c) Jockusch, R. A.; Schnier, P. D.; Price, W. D.; Strittmatter, E. F.; Demirev, P. A.; Williams, E. R. *Anal. Chem.* **1997**, *69*, 1119. (d) Price, W. D.; Schnier, P. D.; Williams E. R. *J. Phys. Chem.* **1997**, *101*, 664.

(11) See, for example: (a) Beyer, M.; Berg, C.; Görlitzer, H. W.; Schindler, T.; Achatz, U.; Albert, G.; Niedner-Schatteburg, G.; Bondybey, V. E. *J. Am. Chem. Soc.* **1996**, *118*, 7386. (b) Beyer, M. Achatz, U.; Berg, C.; Joos, S.; Niedner-Schatteburg, G.; Bondybey, V. E. *J. Phys. Chem. A* **1999**, *103*, 671. (c) Fox, B. S.; Beyer, M. K.; Bondybey, V. E. *J. Phys. Chem. A* **2001**, *105*, 6386. (d) Lee, S.-W.; Freivogel, P.; Schindler, T.; Beauchamp, J. L. *J. Am. Chem. Soc.* **1998**, *120*, 11758. (e) Lee, S.-W.; Chang, S.; Kossakovski, D.; Cox, H.; Beauchamp, J. L. *J. Am. Chem. Soc.* **1999**, *121*, 10152.

(12) Aaserud, D. J.; Guan, Z.; Little, D. P.; McLafferty, F. W. *Int. J. Mass Spectrom. Ion Processes* **1997**, *167*/*168*, 705.

(13) Sena, M.; Riveros, J. M. *Rapid Commun. Mass Spectrom.* **1994**, *8*, 1031.

(14) Sena, M.; Riveros, J. M. *J. Phys. Chem. A* **1997**, *101*, 4384.

(15) Riveros, J. M.; Sena, M.; Guedes, G. H.; Xavier, L. A.; Slepetys, R. *Pure Appl. Chem.* **1998**, *70*, 1969.

(16) Sena, M.; Riveros, J. M. *Chem. Eur. J.* **2000**, *6*, 785.

(17) Sena, M.; Riveros, J. M. *Adv. Mass Spectrom.* **2001**, *15*, 783.

(18) Sena, M. Doctoral Thesis, Institute of Chemistry, University of São Paulo, São Paulo, Brazil, 2001.

(19) Isomeric mixtures of ions have also been distinguished on the basis of dissociation rate constants under the influence of blackbody radiation. See Schnier, P. D.; Williams, E. R. *Anal. Chem.* **1998**, *70*, 3033.

(20) (a) Meyerson, S.; Rylander, P. N. *J. Am. Chem. Soc.* **1957**, *79*, 1058. (b) Bursey, M. M.; McLafferty, F. W. *J. Am. Chem. Soc.* **1966**, *88*, 529. (c) Budzikiewicz, H.; Djerassi, C.; Williams, D. H. *Mass Spectrometry of Organic Compounds*; Holden-Day, Inc.: San Francisco, CA, 1967; pp 162−169.

(21) (a) Morgon, N. H.; Linnert, H. V.; Giroldo, T.; Riveros, J. M. *J. Phys. Chem.* **1996**, *100*, 18048. (b) Silva, M. L. P.; Riveros, J. M. *Int. J. Mass Spectrom. Ion Processes* **1997**, *165*/*166*, 83. (c) Xavier, L. A.; Riveros, J. M. *Int. J. Mass Spectrom. Ion Processes* **1998**, *179*/*180*, 223.

(22) Frisch, M. J.; Trucks, G. W.; Schlegel, H. B.; Scuseria, G. E.; Robb, M. A.; Cheeseman, J. R.; Zakrzewski, V. G.; Montgomery, J. A.; Stratmann, R. E.; Burant, J. C.; Dapprich, S.; Millam, J. M.; Daniels, A. D.; Kudin, K. N.; Strain, M. C.; Farkas, O.; Tomasi, J.; Barone, V.; Cossi, M.; Cammi, R.; Mennucci, B.; Pomelli, C.; Adamo, C.; Clifford, S.; Ochterski, J. W.; Petersson, G. A.; Ayala, P. Y.; Cui, Q.; Morokuma, K.; Malick, D. K.; Rabuck, A. D.; Raghavachari, K.; Foresman, J. B.; Cioslowski, J.; Ortiz, J. V.; Stefanov, B. B.; Liu, G.; Liashenko, A.; Piskorz, P.; Komaromi, I.; Gomperts, R.; Martin, R. L.; Fox, D. J.; Keith, T.; Al-Laham, M. A.; Peng, C. Y.; Nanayakkara, A.; Gonzalez, C.; Challacombe, M.; Gill, P. M. W.; Johnson, B. G.; Chen, W.; Wong, M. W.; Andres, J. L.; Head-Gordon, M.; Replogle, E. S.; Pople, J. A. *Gaussian 98*, revision A.2; Gaussian, Inc.: Pittsburgh, PA, 1998.

(23) Rabbih, M. A.; Helal, A. I.; Fahmey, M. A. *Indian J. Pure Appl. Phys.* **1981**, *19*, 335.

(24) McLoughlin, R. G.; Traeger, J. C. *Org. Mass Spectrom.* **1979**, *14*, 434.

(25) Centineo, G.; Fragala, I.; Bruno, G.; Spampinato, S. *J. Mol. Struct.* **1978**, *44*, 203.

(26) See, for example: (a) Turecek, F. In *The Chemistry of Enols*; Rappoport, Z., Ed.; John Wiley & Sons: New York, 1990; pp 95−146. (b) Schwarz, H. *Adv. Mass Spectrom.* **1985**, *10*, 13. (c) Bouchoux, G. *Mass Spectrom. Rev.* **1988**, *7*, 1. (d) Bouchoux, G. *Mass Spectrom. Rev.* **1988**, *7*, 203.

(27) van der Rest, G.; Chamot-Rooke, J.; Nedev, N.; Mourgues, P.; Audier, H. E. *Int. J. Mass Spectrom.* **2000**, *195*, 385.

(28) Kukol, A.; Streble, F.; Thielking, G.; Grützmacher, H. F. *Org. Mass Spectrom.* **1993**, *28*, 1107.

(29) Sena, M.; Riveros, J. M., manuscript in preparation.

(30) Rate constants were obtained under similar conditions by fitting the kinetics of disappearance to a pseudo-single-exponential decay. At low ionizing energies, where proton transfer amounts 10−15%, adjusting the decay to a double exponential can lead to unrealistic values unless the fitting is subjected to artificial constraints. At higher ionization energies, where proton transfer becomes significant, the kinetic curves are well-described by a double exponential decay.

(31) Rabbih, M. A.; Selim, E. T. M. *Org. Mass Spectrom.* **1980**, *15*, 195.

(32) (a) Das, P. K.; Encinas, M. V.; Small, R. D.; Scaiano, J. C. *J. Am. Chem. Soc.* **1979**, *101*, 6965. (b) Haag, R.; Wirz, J.; Wagner, P. J. *Helv. Chim. Acta* **1977**, *60*, 2595.

(33) Marcinek, A.; Michalak, J.; Rogowski, J.; Tang, W.; Bally, T. *J. Chem. Soc., Perkin Trans. 2* **1992**, 1353.

(34) Schwarz, H. *Top. Curr. Chem.* **1978**, *73*, 232.

(35) Barkow, A.; Pilotek, S.; Grützmacher, H. F. *Eur. Mass Spectrom.* **1995**, *1*, 525.

(36) Moraes, L. A. B.; Pimpim, R. S.; Eberlin, M. N. *J. Org. Chem.* **1996**, *61*, 8726.

(37) Moraes, L. A. B.; Eberlin, M. N. *J. Am. Soc. Mass Spec.* **2001**, *12*, 150.

(38) Mourgues, P.; Denhez, J. P.; Audier, H. E.; Hammerum, S. *Org. Mass Spectrom.* **1993**, *28*, 193.

(39) Chamot-Rooke, J.; van der Rest, G.; Mourgues, P.; Audier, H. E. *Int. J. Mass Spectrom.* **2000**, *195*/*196*, 385.

(40) Stirk, K. M.; Orlowski, J. C.; Leeck, D. T.; Kenttämaa, H. I. *J. Am. Chem. Soc.* **1992**, *114*, 8604.

(41) Although a value of 8.18 ± 0.03 eV was determined by photoionization (Li, W.-K.; Chiu, S.-W.; Ma, Z.-X.; Liao, C. L.; Ng, C. Y. *J. Chem. Phys.* **1993**, *99*, 8440), a much lower value of 7.4 eV has been recommended for the IE of MeSSMe from an evaluation of existing data. See: NIST Standard Reference Database Number 69, July 2001 Release, http://webbook.nist.gov/chemistry/.

(42) Ryan, M. F.; Eyler, J. R.; Richardson, D. E. *J. Am. Chem. Soc.* **1992**, *114*, 8611.

(43) Bar, R.; Heinis, T.; Nager, C.; Jungen, M. *Chem. Phys. Lett.* **1982**, *91*, 440.

(44) Optimized geometries are available upon request from the authors.

(45) Gambi, A.; Giorgani, S.; Passerini, A.; Visinoni, R.; Ghersetti, S. *Spectrochim. Acta* **1980**, *36A*, 871.

(46) Holmes, J. L.; Lossing, F. P. *J. Am. Chem. Soc.* **1980**, *102*, 1591.

(47) Heydorn, L. N.; Ling, Y.; Oliveira, G.; Martin, J. M. L.; Lifshitz, C.; Terlouw, J. K. *Z. Phys. Chem. (Munich)* **2001**, *215*, 141.

(48) See, for example: Heinrich, N.; Louage, F.; Lifshitz, C.; Schwarz, H. *J. Am. Chem. Soc.* **1988**, *110*, 8183.

(49) Grellman, K. H.; Weller, H.; Tauer, E. *Chem. Phys. Lett.* **1983**, *95*, 195.

(50) See, for example: Bombach, R.; Dannacher, J.; Stadelman, J. P. *J. Am. Chem. Soc.* **1983**, *105*, 4205.

(51) (a) Andrews, L.; Keelan, B. W. *J. Am. Chem. Soc.* **1981**, *103*, 99. (b) Lifshitz, C.; Gotkis, Y.; Ioffe, A.; Laskin, J.; Shaik, S. *Int. J. Mass Spectrom. Ion Processes* **1993**, *125*, R7. (c) Rebrion-Rowe, C.; Mostefaoui, T.; Laubé, S.; Mitchell, J. B. A. *J. Chem. Phys.* **2000**, *113*, 3039.